5ICEGE
5th International Conference on Earthquake Geotechnical Engineering
January 2011, 10-13 | Santiago, Chile
Paper No. CSAUB

CENTRIFUGE SCALING ANALYSIS OF PILE RESPONSE TO LATERAL SPREADING MODELS

Javier Ubilla[1], Tarek Abdoun[2], Ricardo Dobry[3]

ABSTRACT

This paper presents the results of centrifuge tests modeling the single pile interaction with liquefied sand conducted at Rensselaer Polytechnic Institute (RPI) in Troy, New York. A critical analysis of the scaling laws currently used for this kind of centrifuge tests is included, focusing in the use of viscous fluid for centrifuge model saturation and the validity of the centrifuge scaling laws when shear band development plays an important role soil-structure interaction.

Keywords: Centrifuge, Scaling Law, Piles, Lateral Spreading, Liquefaction, Shear Band

INTRODUCTION

Soil liquefaction and lateral spreading are one of the main causes of damage of bridges and port facilities during earthquakes, producing distress to piles and other deep foundations (Mizuno, 1987; Dobry and Abdoun, 2001; Ishihara, 2003, Boulanger et al., 2003; Tokimatsu et al., 2005). Such damage can have drastic consequences, impeding emergency response and rescue operations in the short term and causing significant economic loss from business disruption in the longer term.

Liquefaction, lateral spreading and pile foundation represent a complex soil-structure interaction problem which is very difficult to model analytically. It involves large ground deformations, both cyclic and permanent, inertial effects during shaking, and soil-foundation and foundation-superstructure interactions, all in the presence of rapidly changing soil properties with time. Centrifuge physical modeling has emerged as an important tool to study the problem, understand and quantify the parameters involved, and provide guidance and calibration to both simplified engineering procedures and numerical simulation techniques (Dobry and Abdoun, 2001).

This paper presents the results of four centrifuge tests modeling pile foundations under lateral spreading loads conducted at the Rensselaer Polytechnic Institute (RPI). Also included is a critical review of the scaling laws commonly used in centrifuge modeling, in particular the scaling of time and the use of viscous fluid for the saturation of models involving piles, liquefaction and lateral spreading.

CENTRIFUGE MODEL

Centrifuge Model Setup

A series of four centrifuge tests were conducted at Rensselaer Polytechnic Institute (RPI). The 40g models represented a single pile embedded in a layer of saturated sand mildly sloped. Figure 1 shows the

[1] Geotechnical Engineer, Golder Associates Ltd., e-mail: javier_ubilla@golder.com
[2] Professor, Department of Civil Engineering, Rensselaer Polytechnic Institute, email: abdout@rpi.edu
[3] Professor, Department of Civil Engineering, Rensselaer Polytechnic Institute, email: dobryr@rpi.edu

laminar box model setup used in all four centrifuge tests, with the only difference being the viscosity of the fluid used for the model saturation varying the equivalent sand permeability. The permeability of the sand at 1 g ranged from $1.28x10^{-2}$ cm/sec to $3.20x10^{-4}$ cm/sec (Table 1).

Table 1. Centrifuge Tests

Test Name	Sand Relative Density [%]	Fluid Viscosity [cp]	Darcy's Permeability [cm/s]
1 cp	40	1 (water)	$1.28x10^{-2}$
7 cp	40	7	$1.83x10^{-3}$
20 cp	40	20	$6.40x10^{-4}$
40 cp	40	40	$3.20x10^{-4}$

Each of the four models was instrumented with strain gages, accelerometers, pore pressure transducers, LVDTs and laser displacement sensors as shown in Figure 1. The stiffness of the equivalent spring at the base of the piles was measured as 25,000 kNm/rad.

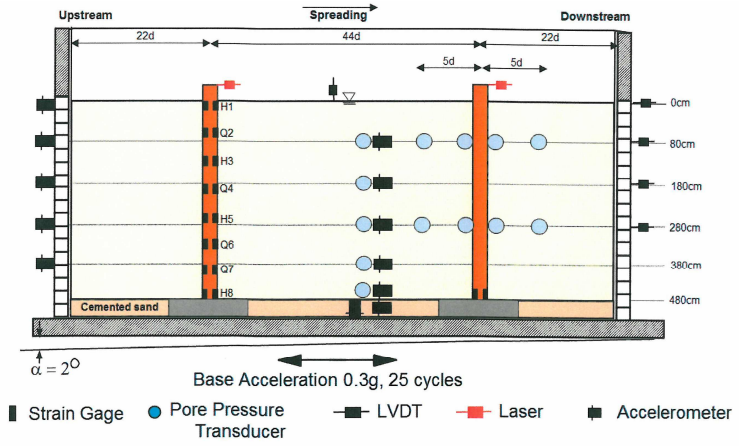

Figure 1. Centrifuge Models Setup

Previous results strongly suggested that the level of excess pore pressures in the soil near the pile is a key factor in the pile bending moment development (Gonzalez et al., 2009). Therefore, special attention was paid to carefully measure the pore pressure around the pile during the lateral spreading. Furthermore, it was considered that the simple placement of a pore pressure transducer near the pile may not measure this phenomenon accurately. This is due to the fact that during shaking and lateral spreading, the sensor would move with the sand and the distance between the sensor and the pile would change.

To address this problem, it was decided to attach the sensor to the pile, so the measurement would always be at the same location relative to the pile during the lateral spreading. On the other hand, it was considered that attaching sensors to the pile may affect the bending moment development during shaking. For that reason, two identical piles were installed in the model, as shown in Figure 1, one located upstream instrumented with strain gages, and the other located downstream, with several pore pressures transducers attached to and around the pile as shown in Figure 1.

In this setup, the upstream pile is used to measure bending moments while the downstream pile is used to measure pore pressure changes around the pile. Figure 2 shows the pore pressure transducers attached to

the pile and those placed at a distance of approximately five pile diameters. These pore pressure sensors were not directly attached to the pile; instead they were attached to a thin and flexible plate glued to the pile in such a way that the sensor could rotate but not translate during lateral spreading, to minimize the influence of the sensor on the pile response during shaking.

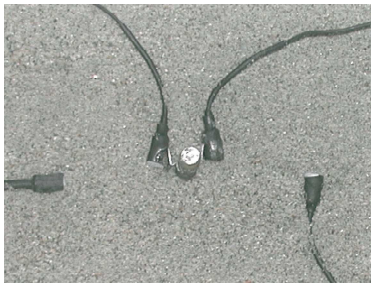

Figure 2. Pore Pressure Transducers around the Pile.

The pile displacement was measured with laser displacement sensors, which produce a very accurate measurement without any physical contact between the sensor and the pile. The prototype input horizontal acceleration at the base of the model consisted of 25 cycles of a sinusoidal wave with an amplitude of 0.3 g and a frequency of 2 Hz. All results presented in this paper are in prototype units, unless otherwise indicated.

Centrifuge Tests Analysis

Pile Response

Figure 3 presents the bending moment profile along the pile and the time histories measured at the bottom of the upstream pile for the four tests listed in Table 1. The bending moments clearly increase as the fluid viscosity goes up and the soil permeability decreases. In general, the pile did not bounce back during the shaking, but for the test 40 cp some reduction of the bending moments at the base was observed toward the end of the shaking, at the time when a huge 780 kNm moment was being measured. It is important to mention that after the shaking and during the pore pressure dissipation the pile did in fact slowly bounce back as shown in Figure 3, where a gradual reduction in bending moment is observed after the shaking.

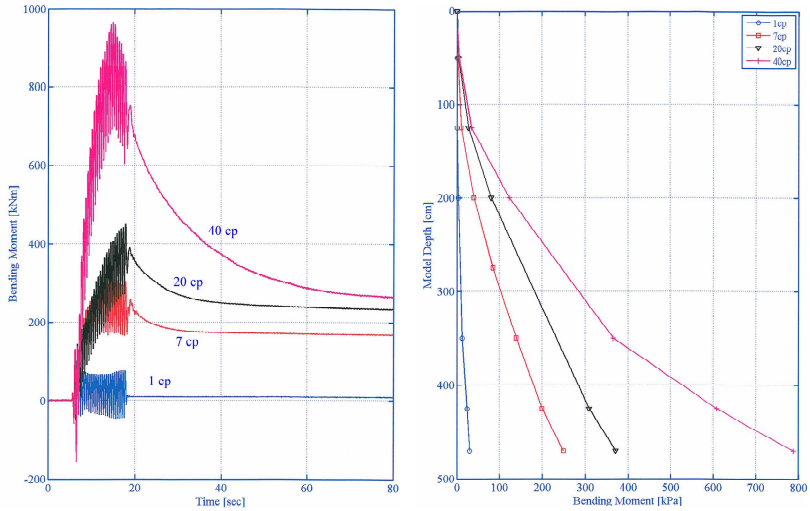

Figure 3. Pile Bending Moments.

The maximum bending moment profiles measured toward the end of the shaking in the upstream pile also increased with the viscosity of the saturating fluid, as shown in Figure 3. Again, the maximum moment, Mmax, always occurred at the bottom of the pile. Changing the fluid viscosity from 1 cp to 40 cp produces a change in the value of Mmax from 30 kNm to 780 kNm. Based on Figure 3, there is strong indication that the fluid viscosity (soil prototype permeability) has a significant influence on pile response. The change in bending moments cannot be attributed to the shear strength of the viscous fluid, as this is about three orders of magnitude smaller than the initial effective stress of the sand (Ubilla, 2007).

Pattern of Soil Deformation and Pore Pressure Development around the Pile

Figure 4 shows time histories of excess pore pressure around the pile for the model 40 cp. Following the commonly used scaling laws, at 40 g centrifugal acceleration this model simulates the prototype soil permeability of the same sand saturated with water (Taylor, 1995).

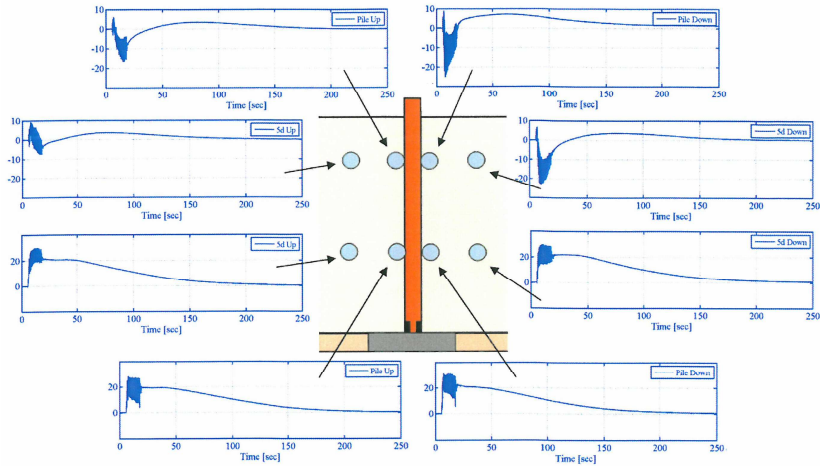

Figure 4. Excess of Pore Pressure in [kPa] Around the Pile.

Figure 4 shows that during lateral spreading, the soil flowing around the pile exhibits a decrease in the excess of pore pressure and therefore an increased effective stress. This indicates that an area of stiff soil has developed around the pile, much stiffer than the liquefied soil in the free field, with this area remaining stiff throughout the shaking. A similar pattern of pore pressure decrease near the pile has been observed in other centrifuge and full scale tests (Suzuki et al. 2005; He et al., 2006; Gonzalez et al., 2009).

In order to better understand this phenomenon, colored markers were placed on a grid around the pile before the centrifuge model saturation. By observing the relative displacements of the makers after shaking, the size and shape of the stiff soil area around the pile could be estimated in the four centrifuge tests. It was observed that the area of influence generated by the pile over the surrounding soil was surprisingly large. This influence area seems to be related to the pore pressure pattern presented in Figure 4. Figure 5 includes pictures taken right after the test showing the typical deformation pattern around the pile for the four models. The deformation pattern of the sand flowing around the pile has an elliptical shape, and the more viscous the saturating fluid the larger is the influence area around the pile.

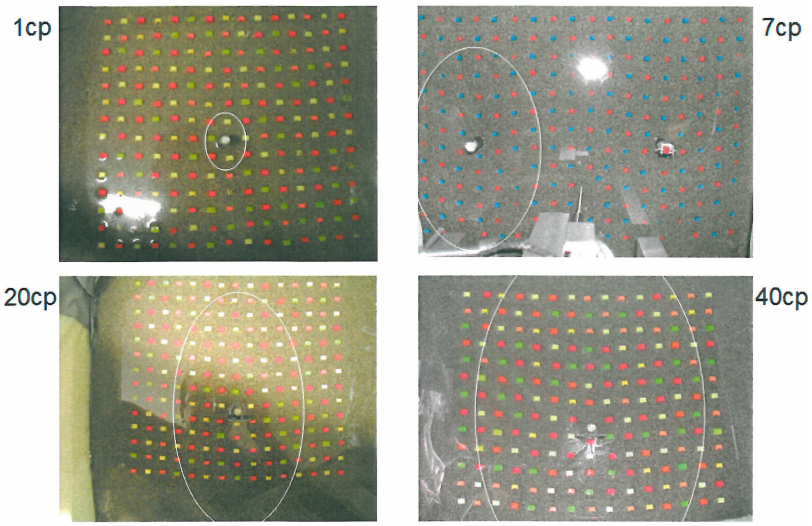

Figure 5. Soil Deformation around the Pile.

Combining this information obtained from the deformation patterns at the ground surface and the pore pressure measurements around the pile, it was possible to estimate the shape of the area of negative excess pore pressure perpendicular to the direction of the spreading. Figure 6 shows that this area has the approximate shape of an inverted triangle. The size of the inverted triangle clearly increases with the viscosity of the fluid. Similar results were reported by Gonzalez et al. (2009).

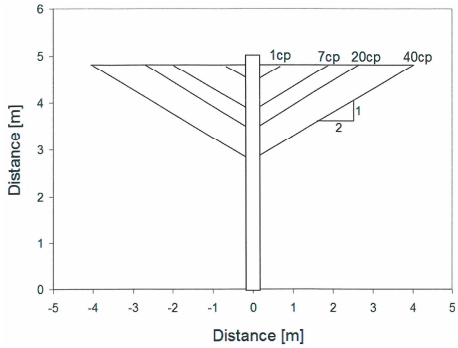

Figure 6. Estimated Shape of Area of Pile Influence.

It is possible to conclude that in such centrifuge models of a single pile subjected to lateral spreading of a uniform sand deposit, a stiffened, non-liquefied area with a inverted triangular shape is developed around the top of the pile. This area is associated with the development of negative excess pore pressures which stiffen the soil around the pile, increasing dramatically the influence area of the pile, which is subjected to the lateral loading by the laterally spreading liquefied soil.

For models saturated with viscous fluid, it was observed that after the shaking the soil in the free field remained liquefied and the soil next to the top portion of the pile remained with negative excess pore pressure, generating a hydraulic gradient towards the pile. As the viscous fluid reached the area next to the pile produced some degree of liquefaction, releasing the grip that the non-liquefied sand had over the pile, and allowed the pile to slowly bounce back towards a new equilibrium position.

THE TIME SCALING LAW

The fundamental scaling law in centrifuge technology is that the distances, dimensions and consequently the amplitudes of any movement in the centrifuge model are scaled down by N times with respect to the prototype.

$$\frac{d_m}{d_p} = \frac{1}{N} \tag{1}$$

Where d is the amplitude of displacement and the subscripts m and p refer to the centrifuge model and prototype respectively.

In a centrifuge model, the acceleration of gravity, g, is increased N times. In order to keep similarity, all accelerations in the model, a_m, are also increased N times with respect to the corresponding acceleration in the prototype a_p.

$$\frac{a_m}{a_p} = N \tag{2}$$

A sinusoidal cyclic movement, x, can be represented as

$$x = d\sin(2\pi ft) \tag{3}$$

Where f is the frequency of the cyclic movement and t is the time.

The acceleration associated with the movement x can be calculated taking double time derivate of Equation 3

$$\ddot{x} = -d(2\pi f)^2 \sin(2\pi ft) \tag{4}$$

Therefore the amplitude of acceleration can be expressed as

$$a = (2\pi f)^2 d \tag{5}$$

Comparing the amplitude of acceleration of the model and prototype and substituting using Equation 2 it is possible to write

$$\frac{a_m}{a_p} = \frac{(2\pi f_m)^2 d_m}{(2\pi f_p)^2 d_p} = \left(\frac{f_m}{f_p}\right)^2 \frac{1}{N} = N \tag{6}$$

Finally, from Equation 6 it is concluded that

$$\frac{f_m}{f_p} = N \quad \text{or} \quad \frac{t_p}{t_m} = N \tag{7}$$

Consequently the scaling law for modeling the dynamic time is N, in other words, for centrifuge tests in which inertial forces is a predominant component, the time in the centrifuge is reduced by N times compared with the prototype. During centrifuge tests of earthquake-induced liquefaction events, certainly inertial forces are an important component of the simulation of the development of liquefaction.

After the earthquake shaking (and often during shaking), the excess pore pressure starts dissipating, with dissipation rate being a function of soil permeability and seepage velocity. If the dissipation occurs too fast the soil recovers its strength before the end of the shaking, while if the dissipation occurs too slowly the soil remains liquefied for a longer period. In the presence of a pile foundation, this phenomenon can have a significant influence of the response of the pile system and the amount of lateral pressure imposed.

The seepage velocity or the velocity of the fluid flowing in the soil voids is governed by Darcy's Law:

$$v = ki \tag{8}$$

Where v is the seepage velocity, k is the permeability and i is the hydraulic gradient.

When the centrifuge model is saturated with water, the seepage velocity in the model is N times faster than in the centrifuge (Schofield, 1980).

$$v_m = k_m i_m = N k_p i_p = N v_p \tag{9}$$

Equation 9 has been confirmed experimentally (Arulanandan et al., 1988). This scaling law for seepage velocity has been accepted and is commonly used.

Given Equation 9, it is possible to calculate the time scaling law associated with pore pressure dissipation that occurs over a distance L.

$$t_m = \frac{L_m}{v_m} = \frac{L_p}{N} \frac{1}{N v_p} = \frac{1}{N^2} t_p \tag{10}$$

Therefore the time scaling law for seepage is N^2.

$$\frac{t_p}{t_m} = N^2 \tag{11}$$

During earthquakes and liquefaction there are at least two physical phenomena that seem to control the soil response: one is the dynamic movement of the model and the other is the pore pressure dissipation controlled by the seepage velocity. It is desirable that a unique time scaling factor applies to both dynamic movement and seepage. As indicated in Equations 7 and 11 when using water as the saturation fluid for both the model and prototype, the scaling factor for dynamic movement and seepage are N and N^2, respectively.

In order to have a unique scaling factor, a saturation fluid of a viscous fluid of N times that of water is commonly used. The definition of intrinsic permeability, K, presented in Equation 12 is fundamental for the development of this theory (Muskat, 1937), even though Equation 12 unrealistically implies that soil permeability is a function of gravity, when in fact it is a function of pressure differential (Taylor, 1995), the equation is widely used,

$$K = \frac{\mu k}{\rho g} \Rightarrow k = \frac{K \rho g}{\mu} \tag{12}$$

Where μ is the dynamic viscosity of the pore fluid, ρ is the mass density of the soil, and g is the acceleration of gravity.

In the centrifuge model, increasing the viscosity of the fluid N times has the effect of reducing N times the soil permeability.

$$k_m^* = \frac{K \rho g}{N \mu} = \frac{k_m}{N} \tag{13}$$

Therefore the new seepage velocity in the model v_m^* would be the same as the seepage velocity in the prototype

$$v_m^* = k_m^* i_m = \frac{k_m}{N} i_m = \frac{N}{N} k_p i_p = v_p \tag{14}$$

As a consequence, the time scaling using viscous fluid is adjusted.

$$t_m = \frac{L_m}{v_m} = \frac{L_p}{N} \frac{1}{v_p} = \frac{1}{N} t_p \tag{15}$$

$$\frac{t_p}{t_m} = N \tag{16}$$

Equations 7 and 16 indicate that a scaling factor on N would properly simulate dynamic movement and seepage velocity when the model is saturated with viscous fluid. The scaling factors associated with centrifuge simulation of earthquake-induced liquefaction and lateral spreading seem consistent.

SHEAR BAND FORMATION AROUND THE PILE

Figure 7 schematically shows the potential for the shear band formation around pile foundation during liquefaction induced lateral spreading. During the similar centrifuge models saturated with water in which full liquefaction was achieved (Abdoun et al, 2003; Ubilla, 2007; Gonzalez et al., 2009), it was observed that after a few cycles the piles bounced back reducing its bending moments while the soil kept flowing around the pile.

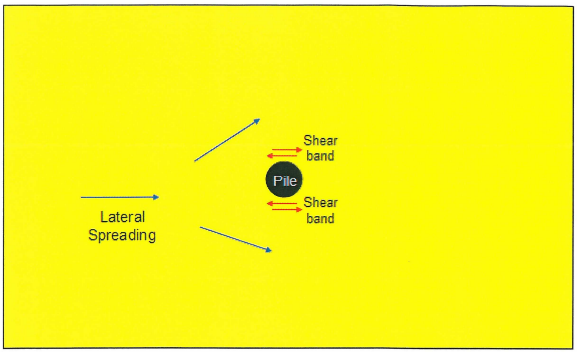

Figure 7. Schematic Shear Band Development.

If the soil flows around the pile there must be a strain discontinuity or shear band that develops in the vicinity of the pile. For centrifuge models saturated with viscous fluid it has been consistently observed that the pile does not bounce back, this means that there is no shear band development around the pile, or perhaps only partial development of such shear banding. This section analyzes the relationship between the shear band development and the use of viscous fluid for model saturation.

Shear banding is the localization of deformation into narrow zones of intense shearing. Shear bands develop in zones of stress concentration, where the granular material tends to reach critical state (Gudehus and Nubel, 2004) and fails developing large strains. When the granular material reaches the critical state or steady state, it will exhibit contractive behavior if it is very loose, a contractive and then dilative behavior if it is medium dense, and a purely dilative behavior if it is dense. According to Sadr et al. (2004), the shear bands dilate during the shear process and reach their maximum volume when the shearing displacement reaches two to three times its shear band thickness.

Using X-rays, Nemat-Nasser and Okada (2001) observed that shear banding can occur within a liquefied sample of a cohesionless granular mass, under cyclic loading. This localization takes place as the liquefied granular mass recovers its effective pressure within a cycle of shearing.

In terms of geometry, shear bands occur over very narrow zones with a thickness between 7 to 20 d_{50}. This thickness seems not to be scalable in centrifuge tests. Wolf et al., (2005) found that the geometry of the shear band pattern is sparsely influenced by the change in the stress level (g level). Wolf et al. studied the shear band formation at 1 g and in centrifuge tests, and they found that the shear band geometry is the same at 1 g, 10 g and 15 g. Also, it has been observed that low permeability delays considerably the growth of the shear band instabilities (Loret and Prevost, 1991). This means that the more viscous the fluid the slower the development of the shear bands.

Undrained dilative behavior seems to be recurrent phenomena associated with earthquake induced liquefaction and lateral spreading observed in centrifuge tests (Gonzalez et al., 2009) and in the field (Elgamal et al, 1998). For medium density sands the shear band formation implies actual volume dilation in the shearing zone with corresponding localized increase in porosity. Figure 8 shows schematically the stages of the shear band formation: before liquefaction and lateral spreading the fluid pressure is positive, then the earthquake induced liquefaction and lateral spreading begins and the soil flows around the pile trying to develop a shear band, at that moment there is a reduction in the pore pressure within the shearing zone around the pile and therefore a seepage gradient is created toward the shearing area. The degree of development of the shear band will depend on how much fluid can actually reach the shearing zone, in other words, it will depend on the seepage velocity of the fluid within the model.

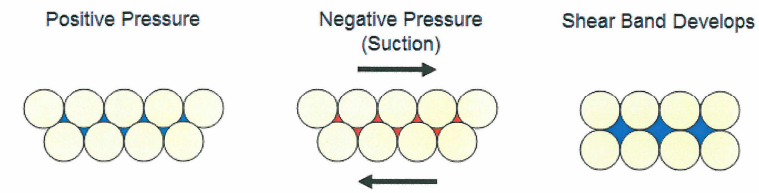

Figure 8. Pore Pressure and Shear Band Development.

Figure 9 shows two elements under shear strain in model and prototype units. As the strain is dimensionless it is the same at 1 g and N g.

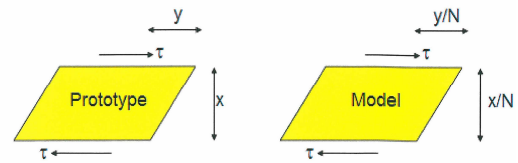

Figure 9. Shear Strain in Prototype and Model Units.

$$\varepsilon_m = \frac{y/N}{x/N} = \frac{y}{x} = \varepsilon_p \tag{18}$$

At the same time, the dynamic time scale is N, or the centrifuge test occurs N times faster than the equivalent prototype. This means that the strain rate, $\dot{\varepsilon}$, in the centrifuge is N times bigger than in the prototype.

$$\dot{\varepsilon}_m = \frac{\varepsilon_m}{t_m} = \frac{y/x}{t_p/N} = \frac{\varepsilon_p}{t_p/N} = N\dot{\varepsilon}_p \tag{19}$$

The shear band is a strain concentration, and the strain rate is N times faster in the centrifuge than in the corresponding prototype. In order to develop the shear band, the viscous fluid needs to reach the shearing zone. The amount of fluid that can reach the shearing zone is a function of the seepage velocity. As a result of using viscous fluid with N times that of the water viscosity to saturate the centrifuge model, the seepage velocity is the same in model and prototype units (Equation 14).

If the same sand having the same density is used in both prototype and centrifuge model, and the soil is subjected to similar straining, the tendency of the soil to dilate and the need for the fluid to fill any tendency for volume increase is expected to be similar. If the centrifuge model is saturated with a viscous fluid having N times the viscosity of water, it will have the same seepage velocity as the prototype. But in the centrifuge the shear band tend to develop N times faster compared to the prototype, which means that the shearing zone in the centrifuge test will have N times less fluid volume available for the development of a shear band. This suggests that the development of the shear band may not be properly scaled in the centrifuge when viscous fluid is used for saturation.

In centrifuge models saturated with viscous fluid, the fact that the sand around the pile cannot actually dilate and produce a shear band, could be a reason for the development of a large solidified soil with negative pore pressure. The solidified soil acts as a stiff area transmitting the lateral pressure of the

liquefied sand to the pile. As the liquefied sand keeps spreading and trying to flow around the pile without being able to develop a shear band, this solidified area keeps increasing in size as the shaking progresses. The size of the solidified area seems to be controlled by the seepage velocity, which could explain the fact that the size of solidified soil seems to be function of the viscosity of the saturation fluid.

From the previous analysis, it is observed that for models saturated with water the seepage velocity is N times faster in the model than in the prototype and, as the shear band development also occurs N times faster, the development of shear banding is correctly modeled. From an engineering point of view, if the goal is to find the maximum bending moments on the pile, the best way to perform these kinds of centrifuge tests may be to saturate the centrifuge model with water. This can be acceptable only in the cases in which the sand is fine enough to keep the models fully liquefied during the shaking.

CONCLUSIONS

There is an inconsistency in the scaling laws currently being used in centrifuge models of liquefaction, lateral spreading and its interaction with pile foundations. The source of this inconsistency is the fact that the bands cannot be scaled. This produces unrealistic results in centrifuge tests, with extremely large bending moments and area of influence of the soil around the pile. More research is needed to find a better way to use centrifuge techniques for modeling this kind of complicated soil structure interaction.

REFERENCES

Abdoun, T., Dobry, R., O'Rourke, T., and Goh, S. (2003). Pile response to lateral spreads: centrifuge modeling. Journal of Geotechnical and Geoenvironmental Engineering, Vol. 129, No. 10, pp. 869-878.

Arulanandan, K., Thompson, P.Y., Kutter, B.L., Meegoda, N.J., Muraleetharan, K.K., and Yogachandran, C. (1988). Centrifuge modeling of transport processes for pollutants in soils. Journal of Geotechnical Engineering, ASCE, 114(2): 185-205.

Boulanger, R.W., Kutter, B.L, Brandenberg, S.J., Singh, P., and Chang, D. (2003). Pile Foundations in Liquefied and Laterally Spreading Ground during Earthquakes: Centrifuge Experiments and Analyses. Report No. UCD/CGM-03/01, Center for Geotechnical Modeling, University of California, Davis, CA, 205 pages.

Dobry, R., and Abdoun, T. (2001). Recent Studies on Seismic Centrifuge Modeling of Liquefaction and its Effect on Deep Foundation. State-of-the-Art Paper, Proc 4th Int Conf on Recent Advances in Geotech Earthq Eng and Soil Dyn (S. Prakash, ed.), Paper SOAP 3, Vol. 2, 30 pages, San Diego, CA, March 26-31.

Elgamal, A., Dobry, R., Parra, E., Zhaohui, Y. (1998). Soil dilation and shear deformations during liquefaction. Proc. 4th Intl. Conf. on Case Histories in Geotechnical Engineering, March 8-15, 1998, Prakash, Ed., St. Louis, Missouri.

Gonzalez, L., Abdoun, T., Dobry, R. (2009). Effect of Soil Permeability on Centrifuge Modeling of Pile Response to Lateral Spreading. Journal of Geotechnical and Geoenvironmental Engineering (ASCE), January 2009.

Gudehus, G., and Nubel, K. (2004). Evolution of shear bands in sand. Geotechnique 54 187–201.

He, L., Elgamal, A., Abdoun, T., Abe, A., Dobry, Meneses, J., Sato, M., and Tokimatsu, K. (2006). Lateral Load on Piles Due to Liquefaction-Induced Lateral Spreading During 1G Shake Table Experiments. Proc. 8th U.S. National Conf on Earthq Eng, April 18-22, San Francisco, CA, Paper No. 881.

Ishihara, K. (2003). Liquefaction-induced lateral flow and its effects on foundation piles. Invited Lecture Fifth National Conference on Earthquake Engineering, May 26-30, Istanbul, Turkey.

Loret, B. and Prevost, J.H. (1991). Dynamic strain localization in fluid-saturated porous media. J. Eng. Mech. ASCE. v117. 907-922.

Mizuno, H. (1987). Pile Damage during Earthquakes in Japan (1923-1983). Proc ASCE Session on Dynamic Response of Pile Foundations (T. Nogami ed.), pp. 53-77, Atlantic City, April 27.

Muskat, M. (1937). The Flow of Homogeneous Fluids through Porous Media. McGraw- Hill Book Company, New York.

Nemat-Nasser, S, Okada, N. (2001). Radiographic and microscopic observation of shear bands in granular materials. Geotechnique 51: 753.

Sadr A., Konagai K., Johansson J., and Yamaguchi, N. (2004). Nonlinear soil-pile group interaction in the vicinity of surface fault ruptures. 13th world conference on earthquake engineering, No.554.

Schofield, A.N. (1980). Cambridge Geotechnical Centrifuge Operations, Geotechnique, Vol. 30, No. 3: 227-268.

Susuki H., Tokimatsu, K., Sato, M., and Abe, A. (2005). Factor Affecting Horizontal Subgrade Reaction of Piles during Soil Liquefaction and Lateral Spreading. ASCE Geotech Special Public No. 145 (Boulanger and Tokimatsu, eds.), Proc Workshop on Seismic Performance and Simulation of Pile Foundations in Liquefiable and Laterally Spreading Ground, March 16-18, University of California, Davis, CA, pp. 1-10.

Taylor, R. N. (1995). Geotechnical Centrifuge Technology, Chapman and Hall, London.

Tokimatsu, K., Suzuki, H., and Sato, M. (2005). Effects of Inertial and Kinematic Interaction on Seismic Behavior of Pile with Embedded Foundation. J of Soil Dyn and Earthq Eng, Vol. 25, pp. 753-762.

Ubilla, J., (2007). Physical Modeling of the Effects of Natural Hazards on Soil-Structure Interaction. PhD thesis. Rensselaer Polytechnic Institute, Troy, NY, USA.

Wolf H, Konig D, Triantafyllidis T. (2005). Centrifuge model tests on sand specimen under extensional load. Int. J. Numer. Anal. Meth. Geomech. 29:25–47.